Differential Deposition of Manganese in the Rat Brain Following Subchronic Exposure to Manganese: a T1-Weighted Magnetic Resonance Imaging Study

Yoram Finkelstein MD PhD[1], Na Zhang PhD[3,9], Vanessa A. Fitsanakis PhD[2], Malcolm J. Avison PhD[4-6,9], John C. Gore PhD[3,4,6,7,9] and Michael Aschner PhD[5,8,10,11]

[1]Neurology and Toxicology Unit and Service, Shaare Zedek Medical Center, Jerusalem, Israel
[2]Department of Biology, King College, Bristol; and Departments of [3]Physics & Astronomy, [4]Radiology & Radiological Sciences, [5]Pharmacology, [6]Neurology, [7]Biomedical Engineering, [8]Molecular Physiology & Biophysics and [9]Pediatrics, [10]Institute of Imaging Science, [11]Center for Molecular Neuroscience and [12]Center of Molecular Toxicology, Vanderbilt University, Nashville, TN, USA

Key words: manganese, magnetic resonance imaging, rodent studies, subchronic exposure, neurotoxicity

Abstract

Background: Manganism is a central nervous system disorder caused by toxic exposure to manganese. Manganism has been related to occupational exposures, liver diseases, prolonged parenteral nutrition, and abuse of illicit drugs. Initially manifested by a reversible neuropsychiatric syndrome (locura manganica), the main symptoms and signs of manganism are emotional lability, compulsive behavior and visual hallucinations. Locura manganica is followed by an irreversible extrapyramidal syndrome, the onset of which occurs years after chronic exposure.

Objectives: To characterize the regional distribution of Mn in the rat brain after subchronic exposure to Mn. This animal model holds special clinical relevance, reflecting the earlier clinical stages of manganism before chronic exposure to Mn exerts its irreversible effects.

Methods: Sprague-Dawley rats were intravenously injected with $MnCl_2$ weekly, for a total of 14 weeks – approximately 1/10 of the lifetime of the rat. T1-weighted magnetic resonance imaging was used to detect the distribution of Mn deposition in brain tissues, as evidenced by areas of T1-weighted hyperintense signals.

Results: A consistent region-specific pattern of T1-weighted hyperintensities was observed in the brains of Mn-treated rats. Cortical hyperintensities were prominent in the hippocampus and dentate gyrus. Hyperintensities were also observed in the olfactory bulbs, pituitary gland, optic nerves and chiasma, pons, midbrain tegmentum, habenula, lentiform and caudate nuclei, thalamus, chorioid plexus and cerebellar hemispheres.

Conclusions: Prominent Mn depositions, evidenced by T1-weighted hyperintensities in the hippocampus after subacute exposure to Mn, are compatible with the clinical picture of manganism during its early stages; and may explain its pathophysiology.

IMAJ 2008;10:793–798

Neurotoxicity of manganese assumes particular clinical relevance in both occupational and environmental medicine. Clinically, manganism is a central nervous system disease and includes a broad spectrum of neurological deficits [1]. The strongest correlation between any type of environmental exposure and increased susceptibility to Parkinson's disease is observed in Mn-exposed populations [2]. It has been estimated that 68,000–185,000 workers in the United States may be exposed to the potential health hazards of Mn and its compounds [3]. There are also numerous reports of Mn intoxication related to long-term total parenteral nutrition [4] and long-term liver failure [5]. Recently, manganism has been observed in intravenous methcathinone abusers in Eastern Europe, where this substance is illicitly produced by a potassium permanganate oxidation process [6]. Methcathinone is an increasingly widely abused and potent synthetic derivative of cathinone [7], the natural amphetamine-like monoamine alkaloid found in leaves of the plant khat (*Catha edulis*), which has long been used in Israel, the Arabian Peninsula, North and Eastern Africa as a psychostimulant..

Initially, patients may complain of anorexia, lassitude and excessive fatigue, apathy, muscle and joint pain. These are followed by signs and symptoms of organic psychosis including impairment of judgment, disorientation, memory loss, compulsive behavior, emotional lability, flight of ideas, visual hallucinations, illusions and delusions. The medical term, locura manganica or manganese madness, describes this initial neuropsychiatric syndrome [1]. Psychomotor slowing and cognitive decline evolve thereafter. This organic brain syndrome is later followed by an extrapyramidal movement disorder with excessive salivation, a disorder clinically resembling Parkinson's disease [8], but with distinct neurological features [9]. The organic psychosis often fades as extrapyramidal signs emerge. Manganism may be reversible if diagnosed and treated in its early stages. The onset of the extrapyramidal signs denotes irreversible damage to the CNS, but these signs appear only after many years of exposure [10]. Occupational exposure to Mn for more than 20 years, or combined long-term exposures to Mn and aluminum for more than 30 years are associated with increased prevalence of Parkinson's disease [2]. Unlike the full-blown syndrome of manganism, which is well characterized by extrapyramidal signs [1,2], little is known about the relationship between manganese and its neuropsychological effects which appear earlier and develop insidiously [11]. The peculiar pattern of delayed toxicity with a biphasic clinical appearance presents a serious challenge when designing animal studies addressing this issue.

Mn = manganese
CNS = central nervous system

MRI and Mn – relevant principles

In order to be measured by MRI, the direction of the net magnetization needs to be tipped away from its equilibrium direction (parallel to the static magnetic field, z-axis). This is carried out by briefly exposing the object to pulses of electromagnetic energy in the form of weak magnetic fields that oscillate at a specific radio frequency which is produced by a transmitter coil. The rotating magnetization produces an oscillating signal within a receiving coil wrapped around the sample. After applying such a radio frequency pulse, the magnetization tends to return to the direction of the original static magnetic field. The time that is associated with the return of longitudinal magnetization to its equilibrium condition is referred to as the spin lattice relaxation time, T1. It reflects the strength and nature of magnetic interactions between the spins and their atomic neighborhood. Divalent Mn ions (Mn +2 oxidation state) have been used as a paramagnetic contrast agent. Given its ability to shorten the T1 time of hydrogen nuclei in water molecules [14] it can be detected by T1-weighted imaging, as tissues with higher Mn levels have shorter relaxation times and demonstrate higher signal intensity in T1-weighted images.

Quantification of the absolute tissue Mn levels is nevertheless problematic, since the relaxivity, a determinant of the relaxation rate, is not an intrinsic property of the Mn ion alone and is subject to change that is dependent on the molecular form of Mn in tissues. It is also likely dependent upon the form in which it is bound [13]. Thus, determining the exact concentrations of Mn in tissues with MRI is problematic. The pallidal index, a comparison of the T1 signal intensity in the globus pallidus to the frontal white matter, has been used to correct for Mn brain depositions [12]; however, the relevance of this calculation to quantitative Mn brain levels must be carefully considered, since Mn also accumulates in brain regions where the denominator is factored in the PI calculation [14].

MRI findings in human brain in manganism

Mn may cause T1-weighted signal hyperintensities in the globus pallidus, striatum and, to a lesser extent, the substantia nigra [15], while idiopathic Parkinson's disease affects mainly the substantia nigra pars compacta and does not cause MRI abnormalities [1]. MRI can also be used to evaluate both the efficacy of various treatment regimens and the effect of cessation of exposure to Mn compounds. Chelation therapy reversed the increases in T1-weighted signal intensity [16], while decreases in the PI have been reported in patients no longer exposed to Mn in occupational settings [13]. There are no reports of MRI abnormalities in humans during the first clinical stages of manganism – the initial stage of non-specific complaints and behavioral changes – and the following stage of neuropsychiatric syndrome (locura manganica).

Mn neurotoxicity and MRI use in rodents

There have been relatively few MRI studies of Mn neurotoxicity. Hyperintensities in rats appear in the choroid plexus and ventricles as the immediate acute effects of exposure to Mn [17]. In mice, dose-dependent Mn-induced hyperintensities were observed in the pituitary gland, olfactory bulb and the hippocampus between 2 and 14 hours after acute exposure [18]. Rat studies demonstrated hyperintensities on T1-weighted MR images after a week of treatment with Mn-fortified parenteral nutrition formula. Cessation of parenteral nutrition treatment for 4 weeks leads to a decrease in these signal intensities [19]. These dynamics are consistent with those observed in human brain MRI following treatment with Mn-fortified PN [12].

The aim of the present MRI study

Review of the pertinent medical literature indicates that MRI abnormalities have been observed first and foremost in the basal ganglia and only in patients with full-blown manganism, clinically manifested by extrapyramidal movement disorder during the late stage of chronic Mn intoxication. On the other hand, MRI studies of manganism in rodent models have focused on the initial acute stages of Mn neurotoxicity and showed a different and possibly reversible pattern of Mn distribution in the CNS. The present MRI study aimed to shed light on the natural progression of Mn neurotoxicity during its early stages, after lengthy exposure to Mn, but still before full-blown Mn neurotoxicity is manifested. In order to characterize the pattern of the regional distribution of Mn in the CNS, rat brains were imaged using T1-weighted MRI after subchronic treatment of the animals with repeated significant intravenous doses of Mn. The duration of exposure was 14 weeks – approximately one-tenth of the lifetime of the rat. This animal model holds special clinical relevance, since manganism is clinically manifested following lengthy periods of exposure to Mn compounds. This rat model of subchronic exposure to Mn may reflect human exposure to Mn for 5–10 years in occupational settings like mining, grinding operations and, possibly, welding. Although 5–10 years is a lengthy period, the full-blown syndrome of manganism is manifested in humans only after a much longer period of exposure to Mn – up to two to three decades. Therefore, it is conceivable that the animal model used in this study may reflect earlier stages of Mn neurotoxicity.

Materials and Methods

The present report focuses on clinical features of Mn-induced neurotoxicity in the rat as part of a multipronged MRI study conducted at Vanderbilt University Medical Center. The original study was designed to test the hypothesis that iron supplementation in the presence of increased Mn exposure leads to decreased brain Mn accumulation [20]. Excerpts of the methodology are briefly recapitulated here.

***Animals*:** All animal protocols were approved by the Vanderbilt University Medical Center Institutional Animal Care and Use Committee. Male Sprague-Dawley rats (ordered from Harlan, Indianapolis, IN), 10–12 weeks old, weight 240–250 g, were supplied with food and water *ad libitum* during the 14 week

MRI = magnetic resonance imaging
PI = pallidal index

experimental protocol. Control (n=5) and Mn-treated (n=6) rats received normal rat chow. In addition, animals from the treatment groups received weekly intravenous tail vessel injections of a sterile isotonic Mn solution (3 mg Mn/kg body mass) of $MnCl_2$ for a total of 14 weeks. Control rats received injections of similar volumes of sterile isotonic saline. Intravenous injected Mn was fully and consistently delivered to the systemic blood circulation, as judged by the measured Mn levels, which were similar in each of the treated rats.

***Blood collection and analysis of* Mn RBC *levels*:** Blood was collected from tail vessels at the conclusion of the study to verify Mn levels. It was collected in heparinized tubes, centrifuged (1000 x g) at 4°C for 30 min to separate red blood cells from plasma and stored at -80°C until Mn analysis by atomic absorption spectroscopy.

For RBCs, a 400 µl aliquot was vortexed with 100 µl 0.5% Triton-X for 30 sec. This was brought up to 1 ml total volume with 2% nitric acid for analysis. The mixture was then centrifuged and the clear supernatant was used for analysis (100 µl aliquot brought up to a 1 ml volume with 2% nitric acid). Bovine liver (10 µg Mn/L) was digested in ultra-pure nitric acid and used as an internal standard for analysis.

MRI: Upon arrival at Vanderbilt, rats were allowed to adjust to their new environment for 4–6 days prior to any handling or testing. Following this, all animals were imaged prior to the beginning of their respective treatment and again at week 14, the last week of the study. In order to maintain consistency during the study, animals were always imaged 24 hours after that week's injection.

For the scans, animals were initially anesthetized with 2% isoflurane and placed in a stereotaxic support cradle with their head secured with tape. The cradle was put in the volume coil to ensure that the rat's head was located in the coil's center. Isoflurane was then lowered to 1.5–1.75% and maintained for the duration of the scanning protocol, usually 1.5 hours. During the scan, body temperature was maintained at 37°C with warm air controlled by a rectal temperature probe (SA Instruments). Respiration was monitored throughout and maintained at 50–70 breaths per minute.

All experiments were acquired using a 4.7 T, 31 cm bore Varian INOVA magnet with actively shielded gradients (40 G/cm, rise time full amplitude of 130 µsec) and a 63 mm transmit/receive quadrature imaging volume coil. Rat brains were scanned from both horizontal (field of view = 40 x 40 mm, 30 slices) and coronal directions (FOV = 40 x 50 mm, 20 slices) with 0.75 mm slice thickness. T1 was measured using 2-D Fast Low Angle Shot sequence (FLASH) with parameters as following: TR/TE = 489/6.59 ms; flip angles = 10, 30, 55 or 70°; 2 acquisitions; image matrix = 256 x 256.

***Image analysis*:** In this study, only raw data are demonstrated, as emphasis is on the clinical attributes associated with the noted effects of Mn accumulation. All animals were scanned at time 0 prior to Mn administration. Each animal was used as its own control.

RBC = red blood cells
FOV = field of view

Results

Blood RBC Mn levels were consistent in all the treated animals, approximately 20 µg/L. The findings on T1-weighted images are consistent in all the examined animals and examples are presented in both coronal and horizontal brain sections [Figures 1,2 and 3,4, respectively). In the Mn-treated group, multiple T1 hyperintensities were evident in specific anatomical structures. The outlines of these structures are well demarcated from their surroundings. Areas showing Mn-associated hyperintensities included hyperintensities (in decreasing order of brightness) in

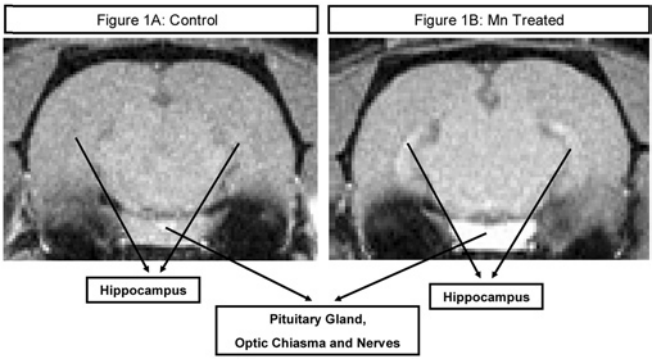

Figure 1. [A] T1-weighted MRI presents a coronal section of a rat brain from the intact control group. No high intensity signals are observed in the brain parenchyma. Tiny foci of high intensity are shown in major blood vessels, out of the brain tissue. **[B]** T1-weighted MRI hyperintense findings are observed at the same level of a rat brain from the Mn-treated group, which received weekly intravenous injections of $MnCl_2$ solution (3 mg Mn/kg body mass) for 14 weeks: bilateral symmetrical high intensity signals sharply demarcate the hippocampi, pituitary gland, optic chiasma and nerves.

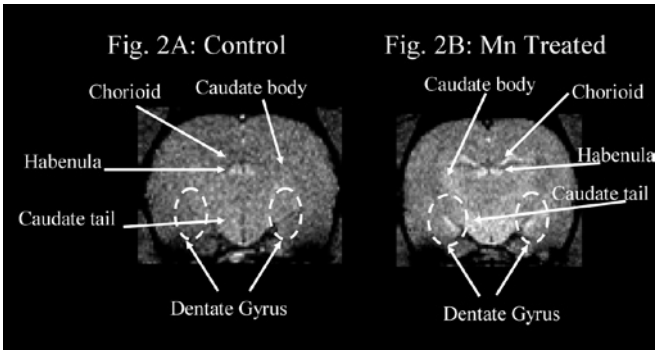

Figure 2. [A] T1-weighted MRI shows a coronal section of a rat brain from the intact control group. No high intensity signals are observed in the brain parenchyma. Tiny foci of high intensity are shown in major blood vessels including the chorioid plexus, and in the habenulae. **[B]** T1-weighted MRI hyperintense findings are observed at the same level of a rat brain from the Mn-treated group, which received weekly intravenous injections of $MnCl_2$ solution (3 mg Mn/kg body mass) for 14 weeks: bilateral symmetrical high intensity signals sharply demarcate the dentate gyri and caudate nuclei. Hyperintense signals are more extensively evidenced in the habenulae and the chorioid plexuses of the Mn-treated rat brain.

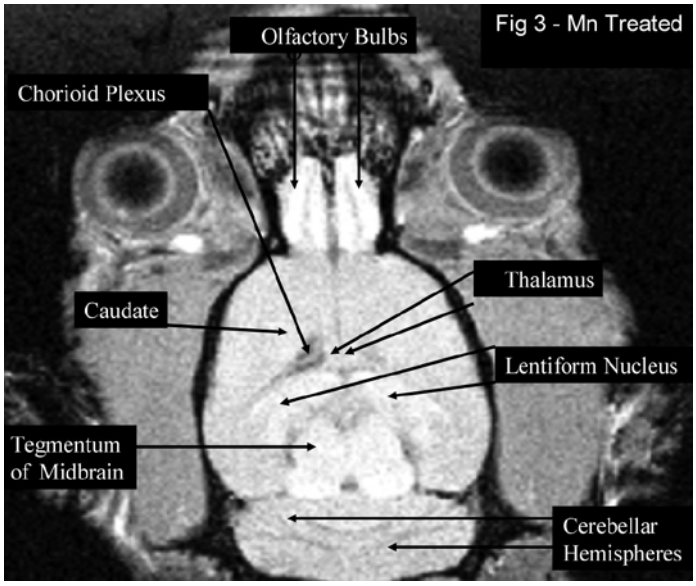

Figure 3. T1-weighted MRI hyperintense findings are observed in a horizontal section of a rat brain from the Mn-treated group, which received weekly intravenous injections of $MnCl_2$ solution (3 mg Mn/kg body mass) for 14 weeks: bilateral symmetrical high intensity signals in the olfactory bulbs, the midbrain tegmentum, the lentiform nucleus which is composed of the globus pallidus and the putamen, the caudate nucleus, the thalamus, the chorioid plexus and the folia of the cerebellar hemispheres (neocerebellum).

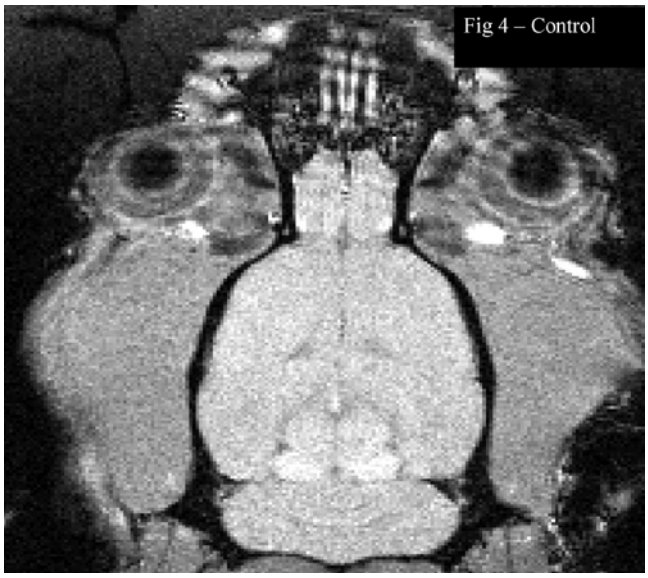

Figure 4. T1-weighted MRI presents a horizontal section of a rat brain from the intact control group, at the same level shown in Figure 3. High intensity signals are observed in the midbrain tegmentum, but less extensively than in the Mn-treated rat brain. Tiny focus of high intensity is shown in the pineal gland in both Figures 3 and 4.

the olfactory bulbs [Figure 3], the pituitary gland [Figure 1B], the optic nerves and optic chiasm [Figure 1B], the hippocampus [Figure 1B] and dentate gyrus [Figure 2B], the pons and midbrain tegmentum [Figure 3], the habenula [Figure 2B], the lentiform nucleus which is composed of the globus pallidus and the putamen [Figure 3], the caudate nucleus [Figures 2B and 3], the thalamus [Figure 3], the chorioid plexus [Figures 2B and 3], and the folia of the cerebellar hemispheres (neocerebellum) [Figure 3]. No locomotor impairment was observed in the animals during the 14 weeks of Mn exposure (data not shown).

In rat brains from the intact control group, at the same levels, high intensity T1-weighted signals are observed in the midbrain tegmentum [Figure 4], but less extensively than in the Mn-treated rat brains. Small foci of high intensity were also evident in the pineal gland [Figure 4], in major blood vessels [Figure 1A], including the chorioid plexus [Figure 2A] and in the habenulae [Figure 2A] – but less extensively than in the Mn-treated rat brains.

Discussion

Mn blood levels in the Mn-treated group reached ~20 µg/L. This level, which is considered two to threefold higher than "normal" values [19], corroborates the concurrent exposure of the rats to Mn. However, it should be emphasized that Mn blood levels may serve merely as an indicator of recent exposure but do not reflect the total body burden of Mn or its intracerebral concentrations.

The T1-weighted MRI images in this study indicate high Mn concentrations in the hippocampal cortex, as well as in other crucial subcortical structures – the brain stem and midbrain, basal ganglia and thalamus. This study also points to significant concentrations of Mn in the olfactory bulbs and the chorioid plexus. The general dispersion of T1 hyperintensities observed throughout the entire brain of Mn-treated rats is similar to the findings of a previous study, performed 1 and 2 weeks after a single i.v. injection of $MnCl_2$, in which radioactive Mn was found ubiquitously throughout the central nervous system, but with the heaviest labeling in hippocampus, thalamus, colliculi, amygdala, olfactory lobe and cerebellum [20]. This likely implies a consistent pattern of distribution of Mn in the CNS, in which the hippocampus and amygadala are significant targets for Mn deposition, at least in the subacute and subchronic stages of exposure.

All animals were scanned at time 0 prior to Mn administration. Furthermore, each animal was used as its own control, so we do have a baseline on which to base our conclusions that Mn treatment led to accumulation of Mn in specific brain regions.

As noted above, Mn was readily deposited in the olfactory bulb area, despite the fact that it was administered by i.v. infusion. This likely reflects the abundance of divalent metal transporter in this area [12]. DMT-1 consists of 17 exons, spanning more than 36 kb and encoding two proteins of 561 and 570 amino acids. DMT-1 has been implicated in the transport of Mn (2+ oxidation state) as well as other divalent metals. In rats, DMT-1 expression is highest in astrocytes and endothelial cells within the striatum, granule and Purkinje cells of the cerebellum, in neurons within the hippocampus and thalamus, and in ependymal cells lining the third ventricle [21,22], with moderate staining in the substantia nigra [23].

DMT-1 = divalent metal transporter

The deposition of Mn in the hippocampus and dentate gyrus, indicated by increased T1-weighted signals, may be relevant to the clinical aspects of manganism. In a recent neurobehavioral study [24], young adult rats exposed subchronically to $MnCl_2$ for 10 weeks demonstrated a dose-dependent increase in glial fibrillary acidic protein immunoreactivity in the hilar part of the dentate gyrus, as well as impairments in spatial memory, exploratory activity and pre-pulse inhibition and diminished sensorimotor reaction. All these neurobehavioral tasks are subserved by the septohippocampal system, suggesting a causal link between Mn-associated deposition and damage to this system. The memory function of initial acquisition, short term (4 hours) and long-term working memory were significantly decreased in the treated animals [24]. Both the septohippocampal system and dentate gyrus play a major role in the acquisition of new information and possibly are an integral neural substrate for spatial reference and spatial working memory [25]. Indeed, these functions might be impaired pursuant to Mn-induced decrease in the activity of the septohippocampal cholinergic system [1]. The septohippocampal cholinergic system also controls spontaneous locomotor activity [26], as observed in rodents that are deficient in M1 muscarinic receptors [27]. The involvement of the hippocampus in the early clinical stages of manganism is crucial, initially in the non-specific complaints and behavioral changes [26] and consequently in the affective disorder of locura manganica [1].

The temporal relationship between hyperintensities in the basal ganglia and the onset of subclinical Mn neurotoxicity has yet to be defined. This is important in determining when metal deposition is actually indicative of a clinical manifestation. This question may be better addressed using non-human primate models of manganism, in which extrapyramidal signs and symptoms are clinically expressed. Additionally, the groundwork for this issue already exists in the present rodent model. A longitudinal MRI study of chronic exposure to Mn will provide information on the long-term dynamics of Mn deposition in the CNS, where the data from human studies suggest that a shift in the pattern of distribution, with increasing basal ganglia hyperintenisities on T1, might presage the emergence of the clinical extrapyramidal stage of manganism.

These observations may assume relevance in the daily clinical toxicology of khat-related substances, the cause of a drug epidemic. Methcathinone was initially patented (but never marketed) by the pharmaceutical firm Parke-Davis in 1957. Subsequently, not later than 1982, it was manufactured by Soviet chemists and became illicitly used worldwide. As estimated, 20% of drug abusers in Russia are addicted to methcathinone [7]. This drug, which is clandestinely synthesized from ephedrine, usually contains Mn as an adulterant from incomplete processing. Therefore, the experimental findings in this animal model may be relevant to numerous intravenous abusers of methcathinone who are prone to manganism.

In conclusion, the present study establishes T1-weighted MRI as a useful tool for determining the relative changes in the deposition of this paramagnetic metal throughout the entire brain. Further work is needed to examine the relationships between the transport of Mn into the brain, the creation of region-specific Mn depositions and the clinical manifestations of manganism.

Acknowledgments: This review was partially supported by grants from NIEHS 10563, DoD W81XWH-05-1-0239, and the Gray E.B. Stahlman Chair of Neuroscience.

References

1. Finkelstein Y, Milatovic D, Aschner M. Modulation of cholinergic systems by manganese. N*eurotoxicology* 2007;28:1003–14.
2. Gorell JM, Johnson CC, Rybicki BA, et al. Occupational exposure to manganese, copper, lead, iron, mercury and zinc and the risk of Parkinson's disease. N*eurotoxicology* 1999;20:239–47.
3. Tanaka S. Manganese and its compounds. In: Zenz C, ed. Occupational Medicine. 32nd edn. St. Louis: Mosby Press, 1994: 213–17.
4. Reimund JM, Dietemann JL, Warter JM, Baumann R, Duclos B. Factors associated to hypermanganesemia in patients receiving home parenteral nutrition. C*lin* N*utr* 2000;19:343–8.
5. Spahr L, Butterworth RF, Fontaine S, et al. Increased blood manganese in cirrhotic patients: relationship to pallidal magnetic resonance signal hyperintensity and neurological symptoms. H*epatology* 1996;24:1116–20.
6. Stepens A, Logina I, Liguts V, et al. A Parkinsonian syndrome in methcathinone users and the role of manganese. N E*ngl* J M*ed* 2008;358:1009–17.
7. Gahlinger PM. Illegal Drugs. New York: Penguin Books, 2004: 231–7.
8. McMillan DE. A brief history of the neurobehavioral toxicity of manganese: some unanswered questions. N*eurotoxicology* 1999;20: 499–507.
9. Bleich S, Degner D, Sprung R, Riegel A, Poser W, Rüther E. Chronic manganism: fourteen years of follow-up. J N*europsychiatry* C*lin* N*eurosci* 1999;11:117.
10. Barbeau A, Inoué N, Cloutier T. Role of manganese in dystonia. A*dv* N*eurol* 1976;14:339–52.
11. Mergler D, Baldwin M. Early manifestations of manganese neurotoxicity in humans: an update. E*nviron* R*es* 1997;73:92–100.
12. Fitsanakis VA, Zhang N, Avison MJ, Gore JC, Aschner JL, Aschner M. The use of magnetic resonance imaging (MRI) in the study of manganese neurotoxicity. N*eurotoxicology* 2006;27:798–806.
13. Kim Y. High signal intensities on T1-weighted MRI as a biomarker of exposure to manganese. I*nd* H*ealth* 2004;42:111–15.
14. Silva AC, Lee JH, Aoki I, Koretsky AP. Manganese-enhanced magnetic resonance imaging (MEMRI): methodological and practical considerations. NMR B*iomed* 2004;17:532–43.
15. Kang YS, Gore JC. Studies of tissue NMR relaxation enhancement by manganese. Dose and time dependences. I*nvest* R*adiol* 1984;19:399–407.
16. Discalzi G, Pira E, Herrero Hernandez E, Valentini C, Turbiglio M, Meliga F. Occupational Mn parkinsonism: magnetic resonance imaging and clinical patterns following CaNa2-EDTA chelation. N*eurotoxicology* 2000;21:863–6.
17. London RE, Toney G, Gabel SA, Funk A. Magnetic resonance imaging studies of the brains of anesthetized rats treated with manganese chloride. B*rain* R*es* B*ull* 1989;23:229–35.
18. Lee JH, Silva AC, Merkle H, Koretsky AP. Manganese-enhanced magnetic resonance imaging of mouse brain after systemic administration of MnCl2: dose-dependent and temporal evolution of T1 contrast. M*agn* R*eson* M*ed* 2005;53:640–8.
19. Chaki H, Furuta S, Matsuda A, et al. Magnetic resonance image and blood manganese concentration as indices for manganese content in the brain of rats. B*iol* T*race* E*lem* R*es* 2000;74:245–57.
20. Fitsanakis VA, Zhang N, Anderson JG, Erikson KM, Avison MJ,

Gore JC, Aschner M. Measuring brain manganese and iron accumulation in rats following 14 weeks of low-dose manganese treatment using atomic absorption spectroscopy and magnetic resonance imaging. *Toxicol Sci* 2008;103:116–24.
21. Gallez B, Baudelet C, Geurts M. Regional distribution of manganese found in the brain after injection of a single dose of manganese-based contrast agents. *Magn Reson Imaging* 1998;16:1211–15.
22. Burdo JR, Menzies SL, Simpson IA, et al. Distribution of divalent metal transporter 1 and metal transport protein 1 in the normal and Belgrade rat. *J Neurosci Res* 2001;66:1198–207.
23. Tandy S, Williams M, Leggett A, et al. Nramp2 expression is associated with pH-dependent iron uptake across the apical membrane of human intestinal Caco-2 cells. *J Biol Chem* 2000;275:1023–9.
24. Gunshin H, Mackenzie B, Berger UV, et al. Cloning and characterization of a mammalian proton-coupled metal-ion transporter. *Nature* 1997;388:482–8.
25. Vezér T, Kurunczi A, Náray M, Papp A, Nagymajtényi L. Behavioral effects of subchronic inorganic manganese exposure in rats. *Am J Ind Med* 2007;50:841–52.
26. Eyre MD, Richter-Levin G, Avital A, Stewart MG. Morphological changes in hippocampal dentate gyrus synapses following spatial learning in rats are transient. *Eur J Neurosci* 2003;17:1973–80.
27. Finkelstein Y, Koffler B, Rabey JM, Gilad GM. Dynamics of cholinergic synaptic mechanisms in rat hippocampus after stress. *Brain Res* 1985;343:314–19.
28. Mattsson A, Pernold K, Ogren SO, Olson L. Loss of cortical acetylcholine enhances amphetamine-induced locomotor activity. *Neuroscience* 2004;127:579–91.

Correspondence: Dr. Y. Finkelstein, Neurology and Toxicology Unit and Service, Shaare Zedek Medical Center, Jerusalem 91031, Israel.
Phone: (972-2) 655-5655
Fax: (972-2) 666-6941
email: yoramf@ekmd.huji.ac.il

Capsule

Autoantibodies to survivin in chronic hepatitis and hepatocellular carcinoma

Previous studies have demonstrated the presence of autoantibodies against tumor-associated antigens, including surviving, in sera from patients with hepatocellular carcinoma. To examine the presence of these antibodies in sera from chronic hepatitis patients, Yagihashi et al., using a recombinant surviving protein in ELISA, studied 57 individuals with chronic hepatitis, 29 with hepatocellular carcinoma, and healthy controls. The study demonstrated that 10 of the 57 patients with chronic hepatitis (17.5%) and 7 of the 29 liver carcinoma patients (24.1%) had these antibodies. Moreover, the authors showed that titers of anti-survivin antibodies were higher in patients with hepatocellular carcinoma associated with hepatitis C virus (HCV) than controls and individuals with this cancer associated with hepatitis B virus infection. On the other hand, no differences were observed regarding anti-survivin in patients with chronic hepatitis caused by HCV and liver carcinoma induced by this virus. This study showed the presence of anti-survivin antibodies in patients with chronic hepatitis and they do not seem to correlate with the progression to hepatocellular carcinoma.

Autoimmunity 2005;38:445

Jozélio Freire de Carvalho

Capsule

Eosinophil structures appear to trap and kill bacterial invaders in the gut

Yousefi et al. suggest that eosinophils serve to protect the gastrointestinal tract from unwanted bacterial invaders, and they do so by engaging an unusual mechanism. Analyzing colon tissue from patients with Crohn's disease, they found that a subset of the infiltrated eosinophils were associated with extracellular structures that contained DNA and eosinophil-derived granule proteins. I*n vitro* studies revealed that when treated with lipopolysaccharide from bacterial pathogens, eosinophils released their mitochondrial DNA in an explosive fashion. This DNA release was dependent on priming of the cells with cytokines and resulted in rapid death of co-cultured bacteria, although the eosinophils themselves remained viable. Mice that had been manipulated genetically to overproduce eosinophils displayed similar extracellular structures in their intestine in response to surgically induced sepsis, and they survived longer than control mice. Thus, these eosinophil-derived structures appear to trap and kill bacterial invaders in the gut. Other researchers had shown previously that neutrophils and mast cells also produce extracellular traps with antimicrobial activity, but in those instances the expelled DNA was nuclear rather than mitochondrial, and that strategy resulted in the death of the immune cells.

Nat Med 2008;14:949

Eitan Israeli